Clim. Past Discuss., 10, 3053–3095, 2014
www.clim-past-discuss.net/10/3053/2014/
doi:10.5194/cpd-10-3053-2014

Climate of the Past Discussions
Open Access

Late Weichselian and Holocene paleoceanography of Storfjordrenna, southern Svalbard

M. Łącka[1], M. Zajączkowski[1], M. Forwick[2], and W. Szczuciński[3]

[1]Institute of Oceanology, Polish Academy of Sciences, Powstańców Warszawy 55, 81-712 Sopot, Poland
[2]Department of Geology, University of Tromsø – The Arctic University of Norway, 9037 Tromsø, Norway
[3]Institute of Geology, Adam Mickiewicz University in Poznan, Maków Polnych 16, 61-606 Poznań, Poland

Received: 15 July 2014 – Accepted: 16 July 2014 – Published: 1 August 2014

Correspondence to: M. Łącka (mlacka@iopan.gda.pl)

Published by Copernicus Publications on behalf of the European Geosciences Union.

Abstract

Multiproxy analyses (incl. benthic and planktonic foraminifera, $\delta^{18}O$ and $\delta^{13}C$ records, grain-size distribution, ice-rafted debris, XRF geochemistry and magnetic susceptibility) were performed on a ^{14}C dated marine sediment core from Storfjordrenna, off southern Svalbard. The sediments in the core cover the termination of Bølling–Allerød, the Younger Dryas and the Holocene, and they reflect general changes in the hydrology/climate of the European Arctic after the last glaciation. Grounded ice of the last Svalbard- Barents Sea Ice Sheet retreated from the coring site ca. 13 850 cal yr BP. During the transition from the sub-glacial to glacimarine setting, Arctic Waters dominated the hydrography in Storfjordrenna. However, the waters were not uniformly cold and experienced several warmer spells. A progressive warming and marked change in the nature of hydrology occurred during the early Holocene. Relatively warm and saline Atlantic Water started to dominate the hydrography from approx. 9500 cal yr BP. Even though the climate in eastern Svalbard was milder at that time than at present (smaller glaciers), there were two slight coolings observed in the periods of 9000–8000 cal yr BP and 6000–5500 cal yr BP. A change of the Storfjordrenna hydrology occurred at the beginning of late Holocene synchronously with glacier growth on land and enhanced bottom current velocities. Although cooling was observed in the surface water, Atlantic Water remained present in the deeper part of water column of Storfjordrenna.

1 Introduction

The northward flowing North Atlantic Current (NAC) is the most important source of heat and salt in the Arctic Ocean (Gammelsrod and Rudels, 1983; Aagaard et al., 1987; Schauer et al., 2004; Fig. 1b). The main stream of Atlantic Water (AW) flowing north to Fram Strait as the West Spitsbergen Current (WSC) causes the dramatic reduction of sea ice extent and thickness through the warming of the intermediate water layer in this region of the Arctic Ocean (Quadfasel et al., 1991; Serreze et al., 2003).

CPD
10, 3053–3095, 2014

Paleoceanographic (e.g., Spielhagen et al., 2011; Dylmer et al., 2013) and instrumental (Walczowski and Piechura, 2006, 2007; Walczowski et al., 2012) investigations provide evidence of a recent intensification of the flow of AW in the Nordic Seas and the Fram Strait.

The Svalbard archipelago is influenced by two water masses: AW flowing northward from the North Atlantic and Arctic Water (ArW) flowing southwest from the northern Barents Sea (Fig. 1b). An oceanic front arising at the contact of different bodies of water is an excellent area to research contemporary and past environmental changes. Intensification of AW flow and associated climate warming cause decreased sea-ice cover in the fjords during winter (Berge et al., 2006), increased sediment accumulation rate (Zajączkowski et al., 2004; Szczuciński et al., 2009) and influences pelage-benthic carbon cycling (Zajączkowski et al., 2010).

Paleoceanographic records indicate that AW was present along the western margin of Svalbard, at least, during the last 12 000 years (e.g. Ślubowska et al., 2007; Werner et al., 2011; Rasmussen et al., 2013); occasionally reaching the Hinlopen Strait and thus transporting warmer and more saline water to the eastern part of Svalbard from the north (Ślubowska-Woldengen et al., 2007; Ślubowska et al., 2008; Kubischta et al., 2010). Periods of enhanced inflow of AW during the Holocene led to the expansion of marine species being absent or only rarely occurring at present. This includes the mollusc *Mytilus edulis* whose fossil remains are widely distributed in raised beach deposits on the western and northern coasts of Svalbard (e.g. Feyling-Hanssen and Jørstad, 1950; Hjort et al., 1992). *Mytilus edulis* spawn at temperatures above 8 to 10 °C (Thorarinsdóttir and Gunnarson, 2003) and thus is considered to indicate higher surface-water temperature related to stronger AW inflow during the early Holocene (11 000–6800 cal yr BP) (Feyling-Hanssen, 1955; Salvigsen et al., 1992; Hansen et al., 2011). Although the progressive development of *Mytilus edulis* is well documented by the periods of warming and inflow of AW to Hinlopen Strait, the presence of this species in Storfjorden (W Edgeøya; Fig. 1) is unclear. Hansen et al. (2011) suggested that a small branch of warm AW could have reached eastern Spitsbergen from south at that time.

CPD
10, 3053–3095, 2014

In the 1980s and 1990s, Storfjorden was regarded to be exclusively influenced by the East Spitsbergen Current (ESC), carrying the cold and less saline ArW from the Barents Sea (Quadfasel et al., 1988; Piechura et al., 1996). More recent studies suggested that the hydrography in Storfjorden is affected by the production of brine-enriched shelf waters (e.g., Haarpaintner et al., 2001; Rasmussen and Thomsen, 2009), the creation of a coastal polynya (e.g., Skogseth et al., 2005; Geyer et al., 2010) or the overflow of dense waters to the continental shelf (e.g., Fer et al., 2003). However, hydrological data obtained from conductivity–temperature sensors attached to a beluga whale showed a substantial and topographically steered inflow of AW to Storfjorden through the Storfjordrenna (Lydersen et al., 2002). Recently, Akimova et al. (2011) reviewed typical water masses for Storfjorden, where the AW was located between 50 and 70 m.

Storfjordrenna is a sensitive boundary area (Fig. 1) where two contrasting water masses form an oceanic polar front, separating colder, less saline and isotopically lighter ArW from warmer, high saline and δ^{18}O heavier AW. An abrupt cooling and warming of the European Arctic might be linked to relatively small displacements of this front (Sarnthein et al., 2003; Hald et al., 2004).

Two sediment cores taken at the mouth of Storfjordrenna, reveal a continuous inflow of AW to the south western Svalbard shelf over the last 20 000 yr with the presence of surface water from 15 000 to 10 000 ^{14}C yr BP (Rasmussen et al., 2007). According to Rasmussen and Thomsen (2009), the isotopic records of δ^{18}O and δ^{13}C in benthic foraminifera tests show low values during cold stadials of the last glaciation, whereas the values from warm periods are higher. Further, the study implies that a light δ^{18}O signal is attributed to brine formation carrying isotopically lighter surface water to the bottom.

In this paper we present results from multi-proxy analyses of a sediment core retrieved 100 km east of the mouth of Storfjordrenna (Fig. 1a). We provide a new age for the retreat of the last Svalbard Barents Sea Ice Sheet from Storfjordrenna and discuss the interaction of oceanography and deglaciation, as well as the postglacial history of Atlantic Water inflow onto the shelf off southern Svalbard.

CPD
10, 3053–3095, 2014

2 Study area

Storfjorden is an approx. 190 km long and up to 190 m deep glacial trough located between the landmasses of Spitsbergen to the west, Edgeøya and Barentsøya to the east, and the shallow Storfjordenbanken to the south-east (Fig. 1a). It is not a fjord sensu stricto, as the sounds of Heleysundet and Freemansundet to the north and northeast, respectively, connect the head of Storfjorden to the north western Barents Sea. A sill of 120 m depth crosses the mouth of Storfjorden. The 254 km long Storfjordrenna, a continuation of the trough that extends towards the shelf break, is located beyond this sill. Bottom depth along the trough axis varies between 150 m and 420 m (Pedrosa et al., 2011). During the late Weichselian Glacial Maximum, Storfjorden and Storfjordrenna were covered by an ice stream draining the Svalbard Barents Sea Ice Sheet (e.g., Ottesen et al., 2005).

2.1 Water masses

The water column of Storfjorden and Storfjordrenna is composed of two main water masses transported with currents from east and south and mixed waters which are formed locally (Table 1 after Skogseth et al., 2005). Warm and saline Atlantic Water (AW) enters Storfjordrenna in a cyclonic manner (Schauer, 1995; Fer et al., 2003), flowing into the trough parallel to its southern margin and flowing towards the trough mouth along its northern slope. The AW occurs between 50 and 70 m in Storfjorden and extends to a depth of 200 m in Storfjordrenna (Akimova et al., 2011). The origin of AW entering Storfjordrenna is an eastward branch of the North Atlantic Current (NAC) following the topography of the Barents Sea Shelf Break. However, approx. 50 % of AW flowing northward also penetrate into Bjørnøyrenna (Smedsrud et al., 2013; for location see Fig. 1). The AW in Storfjordrenna is cooler and fresher than in Bjørnøyrenna as an effect of distance and mixing processes (O'Dwyer et al., 2001). AW may occasionally propagate even further east of Svalbard, where it fills the depressions below 180 m (Schauer, 1995). Relatively cold Arctic Water (ArW) is transported to Storfjor-

CPD
10, 3053–3095, 2014

den and Storfjordrenna by the East Spitsbergen Current (ESC). The ESC enters the fjord through the tidally influenced sounds of Heleysundet and Freemansundet in the north and northeast (Norges Sjøkartverk, 1988), as well as from the southeast with a coastal current flowing around Edgøya (Loeng, 1991). AW and ArW mix to form Transformed Atlantic Water (TAW), which dominates on the shelf off west Spitsbergen (Svendsen et al., 2002; Table 1). Dense, Brine-enriched Shelf Water (BSW) in Storfjorden is produced through high polynya activity and results from intense formation of sea ice (Haarpaintner et al., 2001; Skogseth et al., 2004, 2005). The BSW fills the fjord to the top of the sill (120 m) and initiates a gravity driven overflow (Quadfasel et al., 1988; Schauer, 1995; Schauer and Fahrbach, 1999; Fer et al., 2003, 2004; Skogseth et al., 2005). BSW is characterized by salinity greater than 34.8 and temperature at or slightly above the freezing point (Table 1). Surface Water (SW) in the upper 50 m is cold and fresh during the autumn and warm and fresh due to ice melting during the summer. In winter, the water column in Storfjorden is homogenized due to wind and tidal mixing and is considered to be close to the freezing point (Skogseth et al., 2005).

3 Material and methods

Multi-proxy analyses of the gravity core JM09-020-GC provided the basis for this study. The core was retrieved with R/V *Jan Mayen* (University of Tromsø – The Arctic University of Norway, UiT) in November 2009 from the Storfjordrenna (76°31489′ N, 19°69957′ E), from a bottom depth of 253 m (Fig. 1a). The coring site was located in an area above the continuous presence of BSW and was selected after an echo-acoustic investigation in order to identify the greatest possible area of flat bottom with minimum disturbance of sediments. Conductivity–temperature–depth (CTD) measurements were performed prior to coring (5 November 2009; Fig. 2a) and in summer 2013 (13 August 2013; Fig. 2b).

Prior to sediment core opening, the magnetic susceptibility (MS) was measured using a loop sensor installed on a GEOTEK Multi Sensor Core Logger at the Depart-

CPD
10, 3053–3095, 2014

ment of Geology, UiT. Core sections were stored in the laboratory for one day before measurements thereby allowing the sediments to adjust to room temperature and to avoid measurement errors related to temperature changes (Weber et al., 1997). X-radiographs and digital images were taken from half of the core to define sedimentary and biogenic structures. Sediment colour was defined according to the Munsell Soil Color Charts (Munsell Products, 2009). Qualitative element-geochemical measurements were performed with an Avaatech X-ray fluorescence (XRF) core scanner using the following settings: 10 kV; 1000 µA; 10 s. measuring time; no filter. Both core halves were subsequently cut into 1 cm slices and transported to the Institute of Oceanology, Polish Academy of Sciences in Sopot for further analyses.

Sediment samples for foraminiferal analyses were freeze-dried, weighed, and wet sieved using sieves with mesh-sizes of 500 µm and 100 µm. Residues were dried, weighted again and then split on a dry micro-splitter. Where possible, at least 300 specimens of foraminifera were counted in every 5 cm of sediment. Species identification under a binocular microscope (Nikon SMZ1500) was supported using classification of Loeblich and Tappan (1987), with few exceptions. pPercentages of the 8 indicator species were applied. The number of species per sample and Shannon–Wiener Index were calculated in the program Primer 6. Benthic foraminiferal abundance and ice-rafted debris (IRD; grains > 500 µm) were counted under a stereo-microscope and expressed as flux values (no. of specimens/grains cm^{-2} ka^{-1}) using the bulk sediment density and sediment accumulation rate.

Stable oxygen and carbon isotope compositions of tests of the infaunal foraminifer species *Elphidium excavatum* f. *clavata* were determined at the Department of Geological Sciences, University of Florida (Florida, USA). All values are calibrated to the PeeDee Belemnite (PDB) scale. In our study we discuss the $\delta^{18}O$ and $\delta^{13}C$ record as a relative measure for changes in the water mass characteristics (temperature–salinity) and/or the supply of meltwater/freshwater to the area. Therefore, we have neither corrected the values for vital effect nor the ice volume changes (Erbs-Hansen et al., 2013).

CPD
10, 3053–3095, 2014

Grain size (< 2 mm) analyses were performed every 1 cm using a Malvern Mastersizer 2000 laser particle analyser and presented as volume percent. To examine relative variability in the near-bottom currents the mean grain size distribution of the < 63 µm fraction was calculated, to avoid effect of ice-rafted coarse fraction. Mean grain size was calculated in the program GRADISTAT 8.0 by the geometric method of moments (Blott and Pye, 2001).

3.1 Age control

The chronology for this study is based on high-precision AMS ^{14}C measurements of fragments from nine calcareous bivalve shells. Bivalve taxonomy was confirmed by Dr. Maria Włodarska-Kowalczuk of the Institute of Oceanology, Polish Academy of Sciences. Measurements were performed in the Poznań Radiocarbon Laboratory, which is equipped with the 1.5 SDH-Pelletron Model "Compact Carbon AMS" (Czernik and Goslar, 2001; Goslar et al., 2004). The surface layer of shells was scraped off to avoid contamination with younger carbonate encrustation. The AMS ^{14}C dates were converted into calibrated ages using the calibration program CALIB 6.1 (Stuiver and Reimer, 1993; Stuiver et al., 2005) and the Marine09 calibration curve (Reimer et al., 2009). The difference ΔR in reservoir age correction of the model ocean and region of Svalbard was reported by Mangerud et al. (2006) to be 105 ± 24 or 111 ± 35; we used the first value; calibrated ages are presented in Table 2. It should be noted that the reservoir age is based on few data points from western Spitsbergen, and the age may be different for the eastern coast. However, no data are available from the latter region.

4 Results

4.1 Modern hydrology

In November 2009 the surface water at the coring site (upper ~ 27 m) had already cooled down (1.24 °C; Fig. 2a). However, its salinity was still low (34.24 °C). Trans-

CPD
10, 3053–3095, 2014

formed AW was observed in the layer between 60 and 160 m. The lowermost part of water column shows gradual cooling reaching a minimum temperature of 0.76 °C near the bottom. The lack of BSW at the bottom indicates gradual water mixing during summer and fall. In August 2013, the surface waters had slightly lower salinity, but the temperature was ∼ 5 °C higher than in November 2009 (Fig. 2b). TAW occupied the same depths as in 2009. However, an almost 50 m thick layer of BSW was present close to the seafloor.

4.2 Age model

The ^{14}C ages and calibrated ages are reported in Table 2. The calibration gives an age distribution, not a single value, so the 2-sigma range presented and Fig. 3 shows age probability distribution curves. Ages of samples generally increase with sediment depth except in the case of one sample: St 20A 39, which provided an older age than the sample below. That shell was most likely re-deposited and was thus not used for the age model. However, because all the samples used for dating were shell fragments, it must be taken into account that it is possible that more samples could be subjected to re-deposition, but on the basis of the available data this is not possible to confirm. The age model is based on assuming linear sediment accumulation rates between data points. The highest probability peaks from calibrated age ranges were used as input values for the model. For the lowermost and uppermost parts of the core, we adopted sediment accumulation rates for the neighbouring parts. It is common to observe the loss of the sediment surface layer during coring with heavy gravity cores. In the case of core JM09-020-GC it is likely that at least the top 40 cm of sediments were lost during coring. This conclusion is supported by analysis of a box corer collected prior to coring (Łącka et al., 2014). The extrapolated age model for the sediment surface is, therefore, 1200 cal yr BP.

CPD
10, 3053–3095, 2014

4.3 Lithology

The core JM09-020-GC is 426 cm long and consists of four lithological units L1 (> 13 400 cal yr BP), L2 (~ 13 400 cal yr BP to ~ 11 500 cal yr BP), L3 (~ 11 500 cal yr BP to ~ 3600 cal yr BP) and L4 (~ 3600 cal yr BP to ~ 1200 cal yr BP). The lithological log was created based on the X-radiographs, grain-size analysis data and foraminiferal flux (Fig. 4). Grains > 2 mm are referred to as "clasts" and are marked in the lithological logs as individual features.

Unit L1 (bottom of the core to ~ 370 cm) consists of compacted massive dark grey (Munsell code 5Y 4/1) sandy mud with various amounts of clasts. Bioturbation and foraminifera were generally absent. However, one shell fragment was found at approx. 395 cm.

Unit L2 (~ 370 cm to ~ 272 cm) contains massive dark grey (5Y 4/1) sandy mud with some coarser material and generally lower amounts of clasts than unit L1. The mean grain size (> 63 µm) ranged from 7–10 µm. The highest IRD flux and Fe/Ca ratio for the entire core occur in this unit. The mass accumulation rate (MAR) is 0.044 g cm^{-2} yr^{-1}. The first signs of bioturbation occur in this unit and the flux of foraminifera increases rapidly up to ~ 6000 individuals cm^{-2} ka^{-1} (Fig. 4).

The unit L3 (~ 272 cm to ~ 113 cm) is composed of massive dark olive grey mud (5Y 3/2) and is characterized by decreasing MAR values (0.019 g cm^{-2} yr^{-1} to 0.002 g cm^{-2} yr^{-1}), moderate sand content and clearly increasing mean grain size (> 63 µm). IRD flux is low and the Fe/Ca ratio decreases. Continuous bioturbation and variable foraminiferal fluxes, with maxima in the intervals 9000–8000 cal yr BP and 6000–5500 cal yr BP, are observed.

The uppermost unit L4 (113 cm to core top) is mostly composed of the same material as the underlying unit. However, the sand content is occasionally higher. MAR increases to 0.024 g cm^{-2} yr^{-1}. The mean grain size (> 63 µm) through this interval is even higher than in L3 and reaches up to 15 µm. The bioturbation continues, numerous

CPD
10, 3053–3095, 2014

shell fragments are presented and foraminifera flux reaches high values throughout the entire unit.

4.4 Foraminiferal fauna

A total of 54 calcareous and 6 agglutinated species were identified. The foraminiferal assemblages were dominated by calcareous fauna. Agglutinated species occurred only in 14 sediment samples, and their abundance did not exceeded 4 %. The only exception is the sample dated to ca. 11 300 cal yr BP (262.5 cm depth) with 25 % of agglutinated foraminiferal fauna. However, in this sample the total foraminifera abundance was low. In general, species richness, number of agglutinated foraminifera, as well as rare and fragile species, increase towards the top of the core. Benthic foraminiferal fauna is dominated by *Elphidium excavatum* f. *clavata*, *Cassidulina reniforme*, *Nonionellina labradorica*, *Melonis barleeanum*, *Islandiella* spp. (*Islandiella norcrossi*/*Islandiella helenae*) and *Cibicides lobatulus*. Percentages of *E. excavatum* f. *clavata* show an inverse relationship to *C. reniforme* with the almost constant dominance of the latter species in the periods: ∼ 12 400 cal yr BP to ∼ 12 000 cal yr BP and ∼ 9600 cal yr BP to ∼ 2800 cal yr BP (Fig. 5). Planktonic foraminifera are represented by three species, *Neogloboquadrina pachyderma* (sinistral), *Neogloboquadrina pachyderma* (dextral) and *Turborotalita quinqueloba.* However, the two later species are very rare. In general, the abundance of planktonic fauna is low in the older parts of the core and slightly increases approx. 10 000 cal yr BP reaching maximum values ca. 2000 cal yr BP (Fig. 6).

Based on the most significant changes in the foraminiferal species abundances, species diversity and δ^{18}O and δ^{13}C in *E. excavatum* f. *clavata* tests the core was divided into the four foraminiferal zones F1-F4: ∼ 13 400 cal yr BP to 11 500 cal yr BP (F1); 11 500 cal yr BP to 9200 cal yr BP (F2); 9200 cal yr BP to 3600 cal yr BP (F3); 3600 cal yr BP to 1200 cal yr BP (F4) (Figs. 5 and 6). Zones correspond to lithological division: the age of unit F4 is the same as L4, units F3 and F2 correspond to L3 and unit F1 is linked to unit L2. In unit L4 foraminifera are rare to absent.

CPD
10, 3053–3095, 2014

Zone F1 is dominated by the opportunistic *E. excavatum* f. *clavata* and *C. reniforme*. High percentages of *C. lobatulus* and *Astrononion gallowayi* occur occasionally. Planktonic foraminifera flux was low at the beginning of this section and completely disappeared for almost 1500 years from approx. 11 500 cal yr BP (Fig. 6). Species richness as well as Shannon–Wiener index show low biodiversity. Furthermore, maxima of δ^{18}O and δ^{13}C occur in this interval.

In zone F2 the contribution of *E. excavatum* f. *clavata* and *C. reniforme* is slightly lower, and *N. labradorica* becomes the most abundant species. There is also an increase in *Islandiella* spp. percentage. Planktonic foraminifera appeared again ca. 10 000 cal yr BP. Biodiversity significantly increased and δ^{18}O reached its minimum value of 2.61 ‰ vs. VPDB approx. 10 000 cal yr BP.

Zone F3 is characterized by the minimum mass accumulation rates of sediment and consequently, low temporal resolution. *C. reniforme* dominates over *E. excavatum* f. *clavata* throughout. *M. barleeanum* has its maximum abundance in this zone, and *N. labradorica* is abundant in the lower parts of this zone, decreasing at approx. 7000 cal yr BP. *Islandiella* spp. increases upcore. Planktonic foraminifera occur in the entire zone, and the fluxes are higher than those of previous units (Fig. 6). Biodiversity remains high in this zone, and δ^{18}O and δ^{13}C remain generally stable, however marked peaks occurred at approx. 6800 cal yr BP, 6500 cal yr BP and 5700 cal yr BP, respectively.

A consistently high foraminiferal flux of up to $\sim$ 4900 no. of specimens cm^{-2} ka^{-1} characterises zone F4. The fluxes of *Islandiella* spp. and *Bucella* spp. increase significantly. Additionally, the fluxes of *C. lobatulus* and *A. gallowayi* increase. However, their abundances are lower than those of zone F2. The percentage of *E. excavatum* f. *clavata* increases slightly while *C. reniforme* decreases. A maximum abundance of planktonic foraminifera occurs in this unit. Foraminifera biodiversity continues to increase towards the core top (up to 2.33; Fig. 6). δ^{18}O and δ^{13}C increase slightly, however, with numerous fluctuations.

CPD
10, 3053–3095, 2014

5 Discussion

Based on the most pronounced changes in sedimentological and foraminiferal data as well as comparison to previous studies from adjacent areas, we have distinguished 5 units in the studied core: a sub-glacial unit (> 13 400 cal yr BP), glacier-proximal unit (13 400 cal yr BP to 11 500 cal yr BP), glacimarine unit I (11 500 cal yr BP to 9200 cal yr BP), glacimarine unit II (9200 cal yr BP to 3600 cal yr BP) and glacimarine unit III (3600 to 1200 cal yr BP).

5.1 Sub-glacial unit (> 13 400 cal yr BP)

The lowermost unit L1 (Fig. 4) was significantly coarser, compacted and devoid of foraminifera, which indicates its likely of sub-glacial origin, i.e., it was deposited beneath an icestream draining parts of the last Svalbard–Barents Ice Sheet (SBIS) through Storfjorden. The SBIS deglaciation occurred as a response to sea-level rise and increased mean annual temperature (Siegert and Dowdeswell, 2002). Rasmussen et al. (2007) noted that the outer part of Storfjordrenna (389 m depth; Fig. 1a) was deglaciated before 16 310 ^{14}C yr BP (18 911–19 591 cal yr BP). The bivalve shell fragment from 395.5 cm in our core suggests that the centre part of Storfjordrenna was ice-free before ~ 13 850 cal yr BP. This indicates that the ~ 100 km long retreat of the grounding line from the shelf break to the central part of Storfjordrenna occurred in approx. 5400 years. The deglaciation of the coasts of east Storfjorden islands, Barentsøya and Edgeøya, which are located over 100 km north from the coring site, occurred some 2600 years later, i.e., 11 200 cal yr BP (recalibrated after Landvik et al., 1995). Siegert and Dowdeswell (2002) noted that, during the Bølling–Allerød warming (ca. 14 700–12 700 cal yr BP), some of the deeper bathymetric troughs (e.g., Bjørnøyrenna) had deglaciated first, forming large embayments of ice around them. Probably, Storfjordrenna was one of such embayments at that time.

CPD
10, 3053–3095, 2014

5.2 Glacier-proximal unit (13 400 cal yr BP to 11 500 cal yr BP)

The transition from a subglacial to the glacimarine setting is observed as a distinct change in sediment colour, several peaks of IRD, decreased amount of clasts and the appearance of foraminifera. The sediment accumulation rate (0.044 g cm^{-2} yr^{-1}) was in the same order of magnitude as modern proximal and central parts of west Spitsbergen fjords (see Szczuciński et al., 2009 for review). Textural and compositional analyses of L2 recorded bimodal grain-size distribution and low abundance of microfossils, suggesting that deposition during the deglaciation occurred from suspension settling from sediment-laden plumes and ice rafting. This unit in our core is limited to ~ 60 cm and is characterized by a lack of bioturbation in its lower part.

The flux of IRD in unit L2 correlates well with the abundance of *C. lobatulus* and *A. gallowayi* (Figs. 4 and 5), which are two epibenthic species that often attach to hard substrate e.g., lithic clasts or bivalve shells (e.g., Hald and Steinsund, 1996) and may indicate stronger near-bottom currents (Østby and Nagy, 1982). As the coring site was likely located proximal to one or several ice fronts during the time of deposition of unit L2 and the mean grain size (> 63 µm) is low (Fig. 4), it is likely that the presence of these epibenthic species reflects abundance of hard substrate (IRD) rather than regional oceanography.

During an early phase of the deglaciation of Storfjorden, the East Spitsbergen Current was still not active, because the ice sheet grounded between Svalbardbanken and Storfjordbanken blocked the passage between eastern and western Svalbard (Rasmussen et al., 2007; Hormes et al., 2013). Thus, the first foraminiferal propagules (juvenile forms) were transported by sea currents from the south and west and settled on the seafloor that was exposed after the retreat of grounded ice. The proximal glacimarine environment affected foraminiferal assemblages and resulted in low species richness, biodiversity and low foraminiferal abundance. Consequently, foraminifera assemblages became dominated by fauna typical for the ice proximal settings: *E. excavatum* f. *clavata*, *C. reniforme* and *Islandiella* spp. (e.g., Hald et al., 2004; Hald and Korsun,

CPD
10, 3053–3095, 2014

1997; Korsun and Hald, 1998, 2000). Dominance of *E. excavatum* f. *clavata* confirms the proximity to the ice sheet, decreased salinity and high water turbidity (e.g., Steinsund, 1994; Korsun and Hald, 1998).

The upper part of unit L2 (ca. 12 800–11 500 cal yr BP) spans the Younger Dryas stadial. Records of marine sediments (e.g., Ślubowska-Woldengen et al., 2007, 2008; Zamelczyk et al., 2012), as well as δ^{18}O records from ice cores (e.g., Dansgaard et al., 1993; Grootes et al., 1993; Mayewski et al., 1993; Alley, 2000) show that the Younger Dryas was characterised by a rapid and short-term temperature decrease. This event was likely driven by weakened North Atlantic Meridional Overturning Circulation, a result of the Lake Agassiz outburst (e.g., Gildor and Tziperman, 2001; Jennings et al., 2006) or interaction between the sea ice and thermohaline water circulation (Broecker, 2006), which led to a reduction of AW transport to the north and a dominance of fresher Arctic Water. Our data shows that heavier δ^{18}O recorded e.g., 12 660 cal yr BP and 12 060 cal yr BP, correlate with reduced to absent IRD fluxes, while the peaks of lighter δ^{18}O, e.g., 12 400 cal yr BP, 12 090 cal yr BP and 11 760 cal yr BP, occurred synchronously with significant enhanced IRD fluxes (Fig. 7). Absence of IRD, occasionally for several decades, might reflect temporarily polar conditions caused by the formation of perennial pack ice in Storfjorden locking icebergs proximal to their calving fronts and preventing their movement over the coring site. On the other hand, warmer periods resulted in massive iceberg rafting and delivery of IRD to Storfjordrenna, thus reflecting more sub-polar conditions. Hydrological variability during Younger Dryas was previously noted in some circum-North Atlantic deep-water records (Elmore and Wright, 2011 and references therein). Moreover, oxygen stable isotopes record from an ice-core GISP2 shows some warmer spells during that time (Stuiver et al., 1995), which coincides with higher ice-rafting in Storfjordrenna (Fig. 7). Our data indicate that the Younger Dryas was not uniformly cold and that at least some warmer spells occurred on eastern Svalbard.

We also conclude that the data on δ^{18}O presented in Fig. 7 reflects temperature variations at the coring site according to the isotopically lighter ArW paleotemperature

CPD
10, 3053–3095, 2014

model. Another explanation of the heavier δ^{18}O periods during the YD could be intermittent inflow of AW. However, this is unlikely to cause the synchronous disappearance of IRD.

5.3 Glacimarine unit I (early Holocene; 11 500 cal yr BP to 9200 cal yr BP)

During the early Holocene foraminiferal fauna, although low in abundance, was dominated by species related to the glacimarine environment (*E. excavatum* and *C. reniforme*; Fig. 5). Increasing species richness and biodiversity of foraminifera point to amelioration of environmental conditions and a progressive increase in the distance to the glacier front (Korsun and Hald, 2000; Włodarska-Kowalczuk et al., 2013). Significant fluctuations of the δ^{18}O and δ^{13}C and increasing abundance of *N. labradorica* and *Islandiella* spp. suggest that Storfjordrenna was under the influence of various water masses at this time (Fig. 6). Comparison of our δ^{18}O record with records from the Storfjorden shelf (400 m depth; Rasmussen et al., 2007; Fig. 1a) and the northern shelf of Svalbard (400 m depth; Ślubowska et al., 2005; Fig. 1b) show that all the records are shifted towards lighter values in the early Holocene (Fig. 8) with the record from our core being the most depleted. We suggest that the records located on the western and northern shelf of Svalbard directly mirror the effect of warmer Atlantic water inflow, while record from Storfjordrenna is under influence of isotopically lighter Arctic Water from the Barents Sea.

According to Kaufman et al. (2004), the early Holocene is characterized by higher summer solar insolation at 60° N (10 % higher than today), leading to a reduction in sea-ice cover (Sarnthein et al., 2003). As ice cover decreased, more solar energy was stored in summer and then re-radiated during the winter (e.g., Gildor and Tziperman, 2001). This process accelerated the ice sheet melting and finally, its retreat towards the fjord heads (Forwick & Vorren, 2009; Jessen et al., 2010; Baeten et al., 2010). Our data suggest that the iceberg calving to Storfjordrenna was significantly reduced or even disappeared approx. 10 800 cal yr BP. However, supply of turbid meltwater from

CPD
10, 3053–3095, 2014

land to the study area still resulted in relatively high sediment accumulation rate. Increasing foraminiferal biodiversity in Storfjordrenna (Fig. 6), as well as the occurrence of the thermophilous mollusk *Mytilus edulis* on western Edgeøya (Salvigsen et al., 1992) suggest that the inflow of AW crossed Storfjordrenna and continued northward to the inner fjord by 9500 cal yr BP. Decrease of the Fe/Ca ratio is suggested to reflect increased productivity in the sea and reduced supply of terrigenous material (Croudace et al., 2006). Mean grain size (> 63 µm; Fig. 4) indicates weaker bottom currents in the beginning and stronger at the end of the early Holocene, which might have been related to the ongoing isostatic uplift of the land masses of Svalbard as well as sea level rise (e.g., Forman et al., 2004).

5.4 Glacimarine unit II (mid Holocene; 9200 cal yr BP to 3600 cal yr BP)

The mid Holocene was characterized by relative stable environmental conditions, low sediment accumulation rates (0.002 g cm^{-2} yr^{-1}) and evanescent delivery of IRD (Fig. 4), reflecting very limited ice rafting and reduced supply of fine-grained material to Storfjordrenna. Low sedimentation rates from our records are assumed to reflect reduced glacial conditions on Svalbard during the mid Holocene (Elverhøi et al., 1995; Svendsen and Mangerud, 1997). In contrast, Hald et al. (2004) noted that in the record from Van Mijenfjorden, an enhanced tidewater glaciation occurred during this period; it was thus argued that IRD is a more reliable indicator of glaciation than sedimentation rates. However, ice rafting in Storfjordrenna was generally low.

Shifts between the dominant species *C. reniforme* and *E. excavatum* f. *clavata* (Fig. 5) reflect environmental/hydrological changes (Erbs-Hansen et al., 2013). The decrease of *E. excavatum* f. *clavata* (percentage and flux) points to the reduction in sea ice cover and the limited significance of Transformed Atlantic Water (Khusid and Polyak, 1989). Furthermore, the increase of *C. reniforme* and *M. barleeanum* points to the constant inflow of less modified AW and reduction in sedimentation (e.g., Schröder-Adams et al., 1990; Bergsten, 1994; Jennings and Helgadóttir, 1994; Hald and Steinsund, 1996; Hald and Korsun, 1997). The relative abundance of *M. barleeanum* (Fig. 5)

CPD
10, 3053–3095, 2014

indicates that environmental conditions in Storfjordrenna were similar to contemporary Norwegian fjords that are dominated by AW with a temperature of 6–8 °C and salinities of 34–35 (Husum and Hald, 2004). High total foraminiferal flux at the beginning of this period, as well as high foraminiferal species richness and biodiversity clearly point to AW conditions. These conclusions are also supported by the heavier $\delta^{18}O$, showing AW dominance and significant reduction in the amount of freshwater and ArW in Storfjordrenna (Fig. 8). The continuous presence of *Mytilus edulis* during the entire mid Holocene points to the reduced inflow of the East Spitsbergen Current on account of the AW inflow (Feyling-Hansen, 1955; Forman, 1990; Salvigsen et al., 1992). Together with our results it is suggested that the main way of AW inflow to the eastern Svalbard may have occurred through Storfjordrenna.

Even though sediment accumulation rates were low, and grain size, as well as geochemical proxies, remain relatively constant during the mid Holocene, the foraminiferal flux (including planktonic foraminifera) increased in two periods: of 9000–8000 cal yr BP and 6000–5500 cal yr BP, respectively (Figs. 4 and 6). In both cases the increase in IRD and *I. norcrossi* fluxes (Fig. 9) was followed by a slight depletion in $\delta^{18}O$ and heavier $\delta^{13}C$ suggesting minor cooling and likely seasonal sea-ice formation leading to beach sediment transport by shore ice. Our observations support earlier studies of the overall mid Holocene shifts towards colder environment and fluctuations in the glacial activity in the Svalbard region (e.g., Sarnthein et al., 2003; Forwick and Vorren, 2007, 2009; Skirbekk et al., 2010; Rasmussen et al., 2012). In particular Forwick et al. (2010) suggested that the Tunabreen glacier in Tempelfjorden area advanced between 6000 and 4000 cal yr BP, Baeten et al. (2010) noted higher glacial activity in Billefjorden approx. 5470 cal yr BP and Ojala et al. (2014) pointed to glacier re-advance or surge in Isvika (Nordaustlandet) ca. 5600 cal yr BP. Our data shows an increased supply of IRD fraction to Storfjordrenna sediment followed by variation of $\delta^{18}O$, however, high flux of *M. barleeanum* (Fig. 5) indicates AW condition in southern Storfjorden throughout the whole mid Holocene. The similar ameliorated condition with consistent AW inflow

CPD
10, 3053–3095, 2014

prevailed over the mid Holocene also in the Kveithola Trough south of Storfjordrenna (Groot et al., 2014).

5.5 Glacimarine unit III (late Holocene; 3600 cal yr BP to 1200 cal yr BP)

The late Holocene is characterized by a gradual increase in sediment accumulation rate followed by numerous sharp peaks of sand content and minor peaks of IRD flux, indicating ice growth on land (compare with e.g. Svendsen and Mangerud, 1997; Hald et al., 2004; Forwick and Vorren, 2009; Kempf et al., 2013), slightly enhanced iceberg calving and/or ice rafting over the core site. The IRD record shows few irregular small peaks in the late Holocene (Fig. 7), which, according to Hass (2002), could be correlated with enhanced sea currents increasing the drift of the icebergs. Forwick et al. (2010) suggested several glacier front fluctuations during the past two millennia in Sassenfjorden and Tempelfjorden (W Spitsbergen), hence we suppose increased iceberg calving occurred at Storfjordrenna during this time. However, increased IRD flux can also reflect deposition related to enhanced shore ice rafting. The latter explanation is in agreement with the high percentage of *Islandiella* spp. during the late Holocene (Fig. 5) as well as with the lighter $\delta^{18}O$ record (Fig. 6) indicating a periodic water freshening as the result of meltwater delivery and/or ArW intrusions from the Barents Sea.

The mean grain size (< 63 µm) increases in late Holocene (Fig. 4) and may indicate stronger bottom current velocities and winnowing of fine grained sediments. Andruleit et al. (2006) observed similar increased erosive activity of bottom currents during late Holocene on the SW Svalbard shelf. This sudden increase in current velocities may be connected with postglacial reorganization of oceanographic conditions, relative lowering of the sea level during the postglacial isostatic rebound and/or more intensive sea-ice formation enhancing formation of BSW, forming seasonal near-bottom dense water mass flowing over the coring site (Andruleit et al., 1996). Nevertheless, this process is still not fully understood.

CPD
10, 3053–3095, 2014

Variable hydrological conditions and most likely strong gradients leading to the formation of hydrological fronts increased nutrient advection/upwelling and biological productivity at the coring site during the late Holocene (see Foraminifera flux in Fig. 4). Our data shows increased fluxes of opportunistic species *E. excavatum* and *C. reniforme*, frontal-zone preferring *N. labradorica* and sea-ice related *Islandiella* spp. Abundant, though variable *M. barleeanum* points to high productivity within the euphotic zone leading to enhanced export of organic material/nutrients to the sea floor. This species has been documented in organic-rich mud within troughs of the Barents Sea (Hald and Steinsund, 1996), as well as in temperate fjords of Norway that are strongly influenced by AW (Husum and Hald, 2004). Our data also shows high *N. pachyderma* flux throughout this unit, reflecting a significant increase of euphotic productivity at the coring site. However, low percentage of dextral specimens point to low sea-surface temperatures (Fig. 6). This is in agreement with Rasmussen et al. (2013), which noted that after ca. 3700 cal yr BP, Atlantic Water was only sporadically present at the surface. Cooling at the sea surface reflects the general trend in the Northern Hemisphere related to orbital forcing and reduction of summer insolation at high latitudes over the late Holocene (Wanner et al., 2008).

The last evidence of AW inflow to Edgøya area based on *M. edulis* is dated to 5000 cal yr BP (Hjort et al., 1995). After that time *M. edulis* remained absent until present days. However, its disappearance can rather be related to the freshening of surface water (Berge at al., 2006) and sea ice forcing as opposed to the extinction of AW in Storfjorden over the late Holocene (Rasmussen et al., 2007).

6 Conclusions

Multi-proxy analyses of one sediment core provide new information about the environmental development of the central part of Storfjordrenna off southern Svalbard since the late Bølling–Allerød. The main conclusions of our study are:

– Central Storfjordrenna was deglaciated before ~ 13 850 cal yr BP.

CPD
10, 3053–3095, 2014

- Between ca. 13 400 to 11 500 cal yr BP, Storfjordrenna remained under the influence of Arctic Water masses with periodical sea-ice cover limiting the drift of icebergs. Nevertheless, at least three peaks of temperature increase during Younger Dryas stadial (12 800–11 500 cal yr BP) presumably led to seasonal disappearance of sea ice and significantly enhanced IRD flux indicating more sub-polar conditions.

- Atlantic Water started to flow onto the shelves off Svalbard and into Storfjorden during the early Holocene leading to a progressive warming and significant glacial melting. From ca. 9500 cal yr BP, the Atlantic Water dominated the water column in Storfjordrenna.

- Environmental conditions off eastern Svalbard remained relatively stable from 9200–3600 cal yr BP with glaciers smaller than those of today. However, some small-scale cooling events (9000–8000 cal yr BP and 6000–5500 cal yr BP) indicate minor fluctuations in climate/hydrology of Storfjordrenna.

- A surface-water cooling and freshening occurred in Storfjordrenna during the late Holocene, synchronously with glacier growth and cooling on land. Even though, AW was still present in the deeper part of Storfjordrenna. The late Holocene in Storfjordrenna has been characterized also by increased bottom currents velocities, however the driving mechanism is not fully understood.

Acknowledgements. The study was supported by the Institute of Oceanology Polish Academy of Science and the Polish Ministry of Science and Higher Education with grant no. NN 306 469938. The ^{14}C dating was funded by Polish Ministry of Science and Higher Education grant No. IP2010 040970. We thank the captain and crew of R/V *Jan Mayen*, as well as the cruise participants, in particular Steinar Iversen, for their help at sea. Trine Dahl and Ingvild Hald are acknowledged for the acquisition of X-radiographs. Tine Rasmussen (UiT) is gratefully acknowledged for sharing the data with us. Katarzyna Zamelczyk (UiT) and Maria Włodarska-Kowalczuk (IOPAS) are thanked for help in planktonic foraminifera (Katarzyna) and bivalves (Maria) determination. Patrycja Jernas (UiT) helped during subsampling of the cores. Master's

CPD
10, 3053–3095, 2014

students from the University of Gdansk Kamila Sobala and Anna Nowicka helped with the Mastersizer2000 analysis. We are highly grateful Renata Lucchi (Istituto Nazionale di Oceanografia e Geofisica Sperimentale, Italy), Reignheid Skogseth (University Centre in Svalbard) and Ilona Goszczko (IOPAS) for the comments on the early version of this manuscript. We are sincerely indebted to Amy Lusher (Galway-Mayo Institute of Technology) for improving the English of this manuscript.

References

Aagaard, K., Foldvik, A., and Hillman, S.: The West Spitsbergen Current: disposition and water mass transformation, J. Geophys. Res., 92, 3778–3784, 1987.

Akimova, A., Schauer, U., Danilov, S., and Núòez-Riboni, I.: The role of the deep mixing in the Storfjorden shelf water plume, Deep-Sea Res. Pt. I, 58, 403–414, 2011.

Alley, R.: The younger Dryas cold interval as viewed from central Greenland, Quaternary Sci. Rev., 19, 213–226, 2000.

Alley, R. B. and Augustdottir, A. M.: The 8k event: cause and consequences of a major Holocene abrupt climate change, Quaternary Sci. Rev., 24, 1123–1149, 2005.

Andruleit, H., Freiwald, A., and Schäfer, P.: Bioclastic carbonate sediments on the southwestern Svalbard shelf, Mar. Geol., 134, 163–182, 1996.

Baeten, N. J., Forwick, M., Vogt, C., and Vorren, T. O.: Late Weichselian and Holocene sedimentary environments and glacial activity in Billefjorden, Svalbard, in: Fjord Systems and Archives, edited by: Howe, J. A., Austin, W. E. N., Forwick, M., and Paetzel, M., Geol. Soc. London Spec. Publ., 344, 207–223, 2010.

Berge, J., Johnsen, G., Nilsen, F., Gulliksen, B., Slagstad, D., and Pampanin, D. M.: The *Mytilus edulis* population in Svalbard: how and why, Mar. Ecol.-Prog. Ser., 309, 305–306, 2006.

Bergsten, H.: Recent benthic foraminifera of a transect from the North Pole to the Yermak Plateau, eastern central Arctic Ocean, Mar. Geol., 119, 251–267, 1994.

Blott, S. J. and Pye, K.: GRADISTAT: a grain size distribution and statistics package for the analysis of unconsolidated sediments, Earth Surf. Proc. Land., 26, 1237–1248, 2001.

Briner, J. P., Bini, A. C., and Anderson, R. S.: Rapid early Holocene retreat of a Laurentide outlet glacier through an Arctic fjord, Nature Geosci., 2, 496–499, 2009.

CPD
10, 3053–3095, 2014

Broecker, W. S.: Was the younger Dryas triggered by a flood?, Science, 312, 1146–1148, doi:10.1126/science.1123253, 2006.
Croudace, I. W., Rindby, A., and Rothwell, R. G.: ITRAX: description and evaluation of a new multi-function X-ray core scanner, Geol. Soc. London Spec. Publ., 267, 51–63, 2006.
Czernik, J. and Goslar, T.: Preparation of graphite targets in the Gliwice Radiocarbon Laboratory for AMS ^{14}C dating, Radiocarbon, 43, 283–291, 2001.
Dansgaard, W., Johnsen, S. J., Clausen, H. B., Dahl-Jensen, D., Gundestrup, N. S., Hammer, C. U. C., Hvidberg, S., Steffensen, J. P., Sveinbjörnsdottir, A. E., Jouzel, J., and Bond, G.: Evidence for general instability of past climate from a 250-kyr ice-core record, Nature, 364, 218–220, doi:10.1038/364218a0, 1993.
Dylmer, C. V., Giraudeau, J., Eynaud, F., Husum, K., and De Vernal, A.: Northward advection of Atlantic water in the eastern Nordic Seas over the last 3000 yr, Clim. Past, 9, 1505–1518, doi:10.5194/cp-9-1505-2013, 2013.
Elmore, A. C. and Wright, J. D.: North Atlantic Deep Water and climate variability during the younger Dryas cold period, Geology, 39, 107–110, 2011.
Elverhøi, A., Svendsen, J. I., Solheim, A., Andersen, E. S., Milliman, J., Mangerud, J., and Hooke, R. L.: Late quaternary sediment yield from the high Arctic Svalbard area, J. Geol., 103, 1–17, 1995.
Erbs-Hansen, D. R., Knudsen, K. L., Olsen, J., Lykke-Andersen, H., Underbjerg, J. A., and Sha, L.: Paleoceanographical development off Sisimiut, West Greenland, during the mid- and late Holocene: a multiproxy study, Mar. Micropaleontol., 102, 79–97, 2013.
Fer, I., Skogseth, R., Haugan, P. M., and Jaccard, P.: Observations of the Storfjorden overflow, Deep-Sea Res. Pt. I, 50, 1283–1303, doi:10.1016/S0967-0637(03)00124-9, 2003.
Fer, I., Skogseth, R., and Haugan, P. M.: Mixing of the Storfjorden overflow (Svalbard Archipelago) inferred from density overturns, J. Geophys. Res., 109, C01005, doi:10.1029/2003JC001968, 2004.
Feyling-Hanssen, R.: Stratigraphy of the marine late-Pleistocene of Billefjorden, Vestspitsbergen, Norsk Polarinst. Skri., 107, 1–186, 1955.
Feyling-Hanssen, R. and Jørstad, F.: Quaternary fossil from the Sassen-area in Isfjorden, west-Spitsbergen (the marine mollusk fauna), Norsk Polarinst. Skri., 94, 1–85, 1950.
Forman, S. L.: Post-glacial relative sea level history of northwestern Spitsbergen, Svalbard, B. Geol. Soc. of America, 102, 1580–1590, 1990.

CPD
10, 3053–3095, 2014

Forman, S. L., Lubinski, D. J., Ingólfsson, Ó., Zeeberg, J. J., Snyder, J. A., Siegert, M. J., and Matishov, G. G.: A review of postglacial emergence on Svalbard, Franz Josef Land and Novaya Zemlya, northern Eurasia, Quaternary Sci. Rev., 23, 1391–1434, 2004.

Forwick, M. and Vorren, T. O.: Holocene mass-transport activity in and climate outer Isfjorden, Spitsbergen: marine and subsurface evidence, Holocene, 17, 707–716, 2007.

Forwick, M. and Vorren, T. O.: Late Weichselian and Holocene sedimentary environments and ice rafting in Isfjorden, Spitsbergen, Palaeogeogr. Palaeocl., 280, 258–274, 2009.

Forwick, M., Vorren, T. O., Hald, M., Korsun, S., Roh, Y., Vogt, C., and Yoo, K.-C.: Spatial and temporal influence of glaciers and rivers on the sedimentary environment in Sassenfjorden and Tempelfjorden, Spitsbergen, in: Fjord Systems and Archives, edited by: Howe, J. A., Austin, W. E. N., Forwick, M., and Paetzel, M., Geol. Soc. London Spec. Pub., 344, 163–193, 2010.

Gammelsrod, T. and Rudels, B.: Hydrographic and current measurements in the Fram Strait, Pol. Res., 1, 115–126, 1983.

Geyer, F., Fer, I., and Smedsrud, L. H.: Structure and forcing of the overflow at the Storfjorden sill and its connection to the Arctic coastal polynya in Storfjorden, Ocean Sci., 6, 401–411, doi:10.5194/os-6-401-2010, 2010.

Gildor, H. and Tziperman, E.: A sea ice climate switch mechanism for the 100 kyr glacial cycles, J. Geophys. Res., 106, 9117–9133, 2001.

Goslar, T., Czernik, J., and Goslar, E.: Low-energy ^{14}C AMS in Poznań Radiocarbon Laboratory, Poland, Nucl. Instrum. Meth. B, 223/224, 5–11, 2004.

Groot, D. E., Aagaard-Sørensen, S., and Husum, K.: Reconstruction of Atlantic water variability during the Holocene in the western Barents Sea, Clim. Past, 10, 51–62, doi:10.5194/cp-10-51-2014, 2014.

Grootes, P. M., Stuiver, M., White, J. W. C., Johnsen, S. J., and Jouzel, J.: Comparison of oxygen isotope records from the GISP2 and GRIP Greenland ice cores, Nature, 366, 552–554, 1993.

Haarpaintner, J., Gascard, J., and Haugan, P. M.: Ice production and brine formation in Storfjorden, Svalbard, J. Geophys. Res., 106, 14001–140013, doi:10.1029/1999JC000133, 2001.

Hald, M. and Korsun, S.: Distribution of modern Arctic benthic foraminifera from fjords of Svalbard, J. Foramin. Res., 27, 101–122, 1997.

Hald, M. and Korsun, S.: The 8200 cal. yr BP event reflected in the Arctic fjord, Van Mijenfjorden, Svalbard, Holocene, 18, 981–990, doi:10.1177/0959683608093536, 2008.

CPD
10, 3053–3095, 2014

Hald, M. and Steinsund, P. I.: Benthic foraminifera and carbonate dissolution in surface sediments of the Barents- and Kara Seas, Surface-sediment composition and sedimentary processes in the central Arctic Ocean and along the Eurasian Continental Margin, Ber. Polarforsch., 212, 285–307, 1996.

Hald, M., Ebbsen, H., Forwick, M., Godtliebsen, F., Khomenko, L., Korsun, S., Olsen, L. R., and Vorren, T. O.: Holocene paleoceanography and glacial history of the West Spitsbergen area, Euro-Arctic margin, Quaternary Sci. Rev., 23, 2075–2088, 2004.

Hansen, J., Hanken, N.-M., Nielsen, J. K., Nielsen, J. K., and Thomsen, E.: Late Pleistocene and Holocene distribution of *Mytilus edulis* in the Barents Sea region and its paleoclimatic implications, J. Biogeogr., 38, 1197–1212, 2011.

Hass, H. C.: A method to reduce the influence of ice-rafted debris on a grain size record from northern Fram Strait, Polar Res., 21, 299–306, 2002.

Hjort, C., Andrielsson, L., Bondevik, S., Landvik, J., Mangerud, J., and Salvigsen, O.: *Mytilus edulis* on eastern Svalbard – dating the Holocene Atlantic Water influx maximum, Lundqua Rep., 35, 171–175, 1992.

Hjort, C., Mangerud, J., Adrielsson, L., Bondevik, S., Landvik, J. Y., and Salvigsen, O.: Radiocarbon dated common mussels *Mytilus edulis* from eastern Svalbard and the Holocene marine climatic optimum, Polar Res., 14, 239–243, 1995.

Hormes, A., Gjermundsen, E. F., and Rasmussen, T. L.: From mountain top to the deep sea – deglaciation in 4-D of the northwestern Barents Sea, Quaternary Sci. Rev., 75, 78–99, 2013.

Husum, K. and Hald, M.: A continuous marine record 8000–1600 cal. yr BP from the Malangenfjord, north Norway: foraminiferal and isotopic evidence, Holocene, 14, 877–887, 2004.

Jennings, A. E. and Helgadottir, G.: Foraminiferal assemblages from the fjords and shelf of Eastern Greenland, J. Foramin. Res., 24, 123–44, 1994.

Jennings, A. E., Knudsen, K. L., Hald, M., Hansen, C. V., and Andrews, J. T.: A mid-Holocene shift in Arctic sea-ice variability on the East Greenland Shelf, Holocene, 12, 49–58, 2002.

Jennings, A. E., Hald, M., Smith, M., and Andrews, J. T.: Freshwater forcing from the Greenland Ice Sheet during the Younger Dryas: evidence from southeastern Greenland shelf cores, Quaternary Sci. Rev., 25, 282–298, 2006.

Jessen, S. P., Rasmussen, T. L., Nielsen, T., and Solheim, A.: A new late Weichselian and Holocene marine chronology for the western Svalbard slope 30 000–0 Cal years BP, Quaternary Sci. Rev., 29, 1301–1312, doi:10.1016/j.quascirev.2010.02.020, 2010.

CPD
10, 3053–3095, 2014

Kaufman, D. S., Ager, T. A., Anderson, N. J., Anderson, P. M., Andrews, J. T., Bartlein, P. J., Brubaker, L. B., Coats, L. L., Cwynar, L. C., Duvall, M. L., Dyke, A. S., Edwards, M. E., Eisner, W. R., Gajewski, K., Geirsdóttir, A., Hu, F. S., Jennings, A. E., Kaplan, M. R., Kerwin, M. W., Lozhkin, A. V., MacDonald, G. M., Miller, G. H., Mock, C. J., Oswald, W. W., Otto-Bliesner, B. L., Porinchu, D. F., Rühland, K., Smol, J. P., Steig, E. J., and Wolfe, B. B.: Holocene thermal maximum in the western Arctic (0–180° W), Quaternary Sci. Rev., 23, 529–560, 2004.

Kempf, P., Forwick, M., Laberg, J. S., and Vorren, T. O.: Late Weichselian – Holocene sedimentary palaeoenvironment and glacial activity in the high-Arctic van Keulenfjorden, Spitsbergen, Holocene, 23, 1605–1616, 2013.

Khusid, T. A. and Polyak, L. V.: Biogeography of benthic foraminifers in the Arctic Ocean, in: Neogenooaya i chetoertichnaya paleookeanologiya PO mikropaleontologicheskim dannym (Neogene and Quaternary paleoceanology based on micropaleontological data), edited by: Barash, M. S., Nauka, Moscow (in Russian), 42–50, 1989.

Knudsen, K. L., Eiríksson, J., and Bartels-Jónsdóttir, H. B.: Oceanographic changes through the last millennium off North Iceland: temperature and salinity reconstructions based on foraminifera and stable isotopes, Mar. Micropaleontol., 54–73, 2012.

Korsun, S. and Hald, M.: Modern benthic foraminifera off tide water glaciers, Novaja Semlja, Russian Arctic, Arctic Alpine Res., 30, 61–77, 1998.

Korsun, S. and Hald, M.: Seasonal dynamics of benthic foraminifera in a glacially fed fjord of Svalbard, European Arctic, J. Foramin. Res., 30, 251–271, 2000.

Kubischta, F., Knudsen, K. L., Kaakinen, A., and Salonen, V.-P.: Late Quaternary foraminiferal record in Murchisonfjorden, Nordaustlandet, Svalbard, Polar Res., 29, 283–297, 2010.

Łącka, M. Zajączkowski, M., Forwick, M., and Szczuciński, W.: The 600-years record of Atlantic Water variability in Storfjordrenna, in preparation, 2014.

Landvik, J. Y., Hjort, C., Mangerud, J., Möller, P., and Salvigsen, O.: The Quaternary record of eastern Svalbard: an overview, Polar Res., 14, 95–103, 1995.

Lloyd, J. M., Park, L. A., Kuijpers, A., and Moros, M.: Early Holocene palaeoceanography and deglacial chronology of Disko Bugt, West Greenland, Quaternary Sci. Rev., 24, 1741–1755, 2005.

Loeblich, A. R. and Tappan, H.: Foraminiferal Genera and Their Classification, Van Nostrand Reinhold, New York, 970 pp., 1987.

CPD
10, 3053–3095, 2014

Loeng, H.: Features of the physical oceanographic conditions of the Barents Sea, Polar Res., 10, 5–18, 1991.
Lubinski, D. J., Forman, S. L., and Miller, G. H.: Holocene glacier and climate fluctuations on Franz Josef Land, Arctic Russia, 80° N, Quaternary Sci. Rev., 18, 85–108, 1999.
Lydersen, C., Nøst, O., Lovell, P., McConell, B., Gammelsrød, T., Hunter, C., Fedak, M., Kovacs, K.: Salinity and temperature structure of a freezing Arctic fjord- monitored by white whales (*Delphinapterus leucas*), Geophys. Res. Lett., 29, 2119, doi:10.1029/2002GL015462, 2002.
Mangerud, J., Bondevik, S., Gulliksen, S., Hufthammer, A. K., and Høisæter, T.: Marine ^{14}C reservoir ages for 19th century whales and molluscs from the North Atlantic, Quaternary Sci. Rev., 25, 3228–3245, 2006.
Mayewski, P. A., Meeker, L. D., Morrison, M. C., Twickler, M. S., Whitlow, S. I., Ferland, K. K., Meese, D. A., Legrand, M. R., and Steffensen, J. P.: Greenland ice core "signal" characteristics: an expanded view of climate change, J. Geophys. Res., 98, 12839–12847, doi:10.1029/93JD01085, 1993.
McCarthy, D. J.: Late Quaternary Ice–ocean Interactions in Central West Greenland, Department of Geography, Durham University, Durham, UK, 2011.
Munsell® Color Geological Rock: Color Chart Revised Washable Edition, 2009.
Norges Sjøkartverk: Den norske los – Arctic pilot, Farvannbeskrivelse, sailing directions, Svalbard–Jan Mayen, Seventh edition, Stavanger, Norwegian Hydrographic Service, Norwegian Polar Institute, 1988.
O'Dwyer, J., Kasajima, Y., and Nøst, O.: North Atlantic water in the Barents Sea opening, 1997 to 1999, Polar Res., 2, 209–216, 2001.
Ojala, A. E. K., Salonen, V.-P., Moskalik, M., Kubischta, F., and Oinonen, M.: Holocene sedimentary environment of a High-Arctic fjord in Nordaustlandet, Svalbard, Pol. Polar Res., 03, 35, 73–98, 2014.
Østby, K. L. and Nagy, J.: Foraminiferal distribution in the Western Barents Sea, recent and quaternary, Polar Res., 1, 55–95, 1982.
Ottesen, D., Dowdeswel, L. J. A., and Rise, L.: Submarine landforms and the reconstruction of fast-flowing ice streams within a large Quaternary ice sheet: the 2500 km-long Norwegian–Svalbard margin (57–80° N), Geol. Soc. Am. Bull., 117, 1033–1050, 2005.
Pedrosa, M. T., Camerlenghi, A., de Mol, B., Urgeles, R., Rebesco, M., Lucchi, R. G., Amblas, D., Calafat, A., Canals, M., Casamor, J. L., Costa, S., Frigola, J., Iglesias, O., La-

CPD
10, 3053–3095, 2014

fuerza, S., Lastras, G., Lavoie, C., Liquete, C., Hidalgo, E. C., Flores, J. A., Sierro, F. J., Carburlotto, A., Grossi, M., Winsborrow, M., Zgur, F., Deponte, D., De Vittor, C., Facchin, L., Tomini, I., De Vittor, R., Pelos, C., Persissinotto, G., Ferrante, N., and Di Curzio, E.: Seabed morphology and shallow sedimentary structure of the Storfjorden and Kveithola trough-mouth fans northwest Barents Sea, Mar. Geol., 286, 1–4, 2011.

Piechura, J.: Dense bottom waters in Storfjord and Storfjordrenna, Oceanologia, 38, 285–292, 1996.

Polyak, L. and Solheim, A.: Late- and post-glacial environments in the northern Barents Sea west of Franz Josef Land, Polar Res., 13, 97–207, 1994.

Quadfasel, D., Rudels, B., and Kurz, K.: Outflow of dense water from a Svalbard fjord into the Fram Strait, Deep-Sea Res., 35, 1143–1150, 1988.

Quadfasel, D. A., Sy, A., Wells, D., and Tunik, A.: Warming in the Arctic, Nature, 350, 6317, doi:10.1038/350385a0, 1991.

Rasmussen, T. L. and Thomsen, E.: Stable isotope signals from brines in the Barents Sea: implications for brine formation during the last glaciation, Geology, 37, 903–906, doi:10.1130/G25543A.1, 2009.

Rasmussen, T. L., Thomsen, E., Slubowska-Woldengen, M., Jessen, S., Solheim, A., and Koc, N.: Paleoceanographic evolution of the SW Svalbard margin (76° N) since 20 000 ^{14}C yr BP, Quaternary Res., 67, 100–114, doi:10.1016/j.yqres.2006.07.002, 2007.

Rasmussen, T. L., Forwick, M., and Mackensen, A.: Reconstruction of inflow of Atlantic Water to Isfjorden, Svalbard during the Holocene: correlation to climate and seasonality, Mar. Micropaleontol., 94–95, 80–90, doi:10.1016/j.marmicro.2012.06.008, 2012.

Rasmussen, T. L., Thomsen, E., Skirbekk, K., Ślubowska-Woldengen, M., Klitgaard Kristensen, D., and Koç, N.: Spatial and temporal distribution of Holocene temperature maxima in the northern Nordic seas: interplay of Atlantic-, Arctic- and polar water masses, Quaternary Sci. Rev., 92, 280–291, doi:10.1016/j.quascirev.2013.10.034, 2013.

Reimer, P. J., Baillie, M. G. L., Bard, E., Bayliss, A., Beck, J. W., Blackwell, P. G., Bronk Ramsey, C., Buck, C. E., Burr, G. S., Edwards, R. L., Friedrich, M., Grootes, P. M., Guilderson, T. P., Hajdas, I., Heaton, T. J., Hogg, A. G., Hughen, K. A., Kaiser, K. F., Kromer, B., McCormac, F. G., Manning, S. W., Reimer, R. W., Richards, D. A., Southon, J. R., Talamo, S., Turney, C. S. M., van der Plicht, J., and Weyhenmeyer, C. E.: IntCal09 and Marine09 radiocarbon age calibration curves, 0–50,000 years cal BP, Radiocarbon, 51, 1111–1150, 2009.

CPD
10, 3053–3095, 2014

Rüther, D., Bjarnadóttir, L., R., Junttila, J., Husum, K., Rasmussen, T. L., Lucchi, R. G., and Andreassen, K.: Pattern and timing of the northwestern Barents Sea Ice Sheet deglaciation and indications of episodic Holocene deposition, Boreas, 41, 494–512, doi:10.1111/j.1502-3885.2011.00244.x, 2012.

Salvigsen, O., Forman, S., and Miller, G.: Thermophilous mollusks on Svalbard during the Holocene and their paleoclimatic implications, Polar Res., 11, 1–10, 1992.

Sarnthein, M., van Kreveld, S., Erlenkeuser, H., Grootes, P. M., Kucera, M., Pflaumann, U., and Sculz, M.: Centennial-to-millennial-scale periodicities of Holocene climate and sediment injections off the western Barents shelf, 75° N, Boreas, 32, 447–461, 2003.

Schauer, U.: The release of brine-enriched shelf water from Storfjord into the Norwegian Sea, J. Geophys. Res.-Oceans, 100, 60515–16028, 1995.

Schauer, U. and Fahrbach, E.: A dense bottom water plume in the western Barents Sea: downstream modification and interannual variability, Deep-Sea Res. Pt. I, 46, 2095–2108, 1999.

Schauer, U., Fahrbach, E., Østerhus, S., and Rohardt, G.: Arctic Warming through the Fram Strait: oceanic heat transport from 3 years of measurements, J. Geophys. Res., 109, C06026, doi:10.1029/2003JC001823, 2004.

Schröder-Adams, C. J., Cole, F. E., Medioli, F. S., Mudie, P. J., Scott, D. B., and Dobbin, L.: Recent Arctic shelf foraminifera: seasonally ice covered areas vs. perennially ice covered areas, J. Foramin. Res., 20, 8–36, 1990.

Serreze, M. C., Maslanik, J. A., Scambos, T. A., Fetterer, F., Stroeve, J., Knowles, K., Fowler, C., Drobot, S., Barry, R. G., and Haran., T. M.: A new record minimum Arctic sea ice and extent in 2002, Geophys. Res. Lett., 30, 1110, doi:10.1029/2002GL016406, 2003.

Siegert, M. J. and Dowdeswell, J. A.: Late Weichselian iceberg, surface-melt and sediment production from the Eurasian Ice Sheet: results from numerical ice sheet modeling, Mar. Geol., 188, 109–127, 2002.

Skirbekk, K., Klitgaard Kristensen, D., Rasmussen, T., Koç, N., and Forwick, M.: Holocene climate variations at the entrance to a warm Arctic fjord: evidence from Kongsfjorden Trough, Svalbard, in: Fjord Systems and Archives, edited by: Howe, J. A., Austin, W. E. N., Forwick, M., and Paetzel, M., Geol. Soc. London Spec. Publ., 344, 289–304, 2010.

Skogseth, R., Haugan, P. M., and Haarpaintner, J.: Ice and brine production in Storfjorden from four winters of satellite and in situ observations and modeling, J. Geophys. Res., 109, C10008, doi:10.1029/2004JC002384, 2004.

CPD
10, 3053–3095, 2014

Skogseth, R., Haugan, P. M., and Jakobsson, M.: Watermass transformations in Storfjorden, Cont. Shelf Res., 25, 667–695, 2005.
Ślubowska, M. A., Koç, N., Rasmussen, T. L., and Klitgaard-Kristensen, D.: Changes in the flow of Atlantic water into the Arctic Ocean since the last deglaciation: evidence from the northern Svalbard continental margin, 80° N, Paleoceanography, 20, 1–16, doi:10.1029/2005PA001141, 2005.
Ślubowska-Woldengen, M., Rasmussen, T. L., Koç, N., Klitgaard-Kristensen, D., Nilsen, F., and Solheim, A.: Advection of Atlantic Water to the western and northern Svalbard shelf since 17,500 cal yr BP, Quaternary Sci. Rev., 26, 463–478, doi:10.1016/j.quascirev.2006.09.009, 2007.
Ślubowska-Woldengen, M., Koç, N., Rasmussen, T. L., Klitgaard-Kristensen, D., Hald, M., and Jennings, A. E.: Time-slice reconstructions of ocean circulation changes on the continental shelf in the Nordic and Barents Seas during the last 16 000 cal yr BP, Quaternary Sci. Rev., 27, 1476–1492, doi:10.1016/j.quascirev.2008.04.015, 2008.
Smedsrud, L. H., Esau, I., Ingvaldsen, R. B., Eldevik, T., Haugan, P. M., Li, C., Lien, V. S., Olsen, A., Omar, A. M., Otterå, O. H., Risebrobakken, B., Sandø, A. B., Semenov, V. A., and Sorokina, S. A.: The role of the Barents Sea in the Arctic climate system, Rev. Geophys, 51, 415–449, 2013.
Spielhagen, R. F., Werner, K, Sørensen, S. A., Zamelczyk, K., Kandiano, E., Budéus, G., Husum, K., Marchitto, T. M., and Hald, M.: Enhanced modern heat transfer to the Arctic by warm Atlantic water, Science, 331, 450–453, doi:10.1126/science.1197397, 2011.
Steinsund, P. I.: Benthic foraminifera in surface sediments of the Barents and Kara seas: modern and late Quaternary applications, Ph.D. thesis, University of Tromsø, 1994.
Stuiver, M. and Reimer, P. J.: Extended ^{14}C database and revised CALIB radiocarbon calibration program, Radiocarbon, 35, 215–230, 1993.
Stuiver, M., Grootes, P. M., and Braziunas, T. F.: The GISP2 ^{18}O climate record of the past 16,500 years and the role of the sun, ocean and volcanoes, Quaternary Res., 44, 341–354, 1995.
Stuiver, M., Reimer, P. J., and Reimer, R. W.: CALIB 5.0. [WWW program and documentation], 2005.
Svendsen, H., Beszczynska-Møller, A., Hagen, J. O., Lefauconnier, B., Tverberg, V., Gerland, S., Ørebæk J. B., Bischof, K., Papucci, C., Zajączkowski, M., Azzolini, R., Bruland, O.,

CPD
10, 3053–3095, 2014

Wiemcke, C., Winther, J.-G., and Dallmann, W.: The physical environment of Kongsfjorden-Krossfjorden, an Arctic fjord system in Svalbard, Polar Res., 21, 133–166, 2002.
Svendsen, J. I. and Mangerud, J.: Holocene glacial and climatic variations on Spitsbergen, Svalbard, Holocene, 7, 45–57, 1997.
Svendsen, J. I., Elverhøi, A., and Mangerud, J.: The retreat of the Barents Sea Ice Sheet on the western Svalbard margin, Boreas, 25, 244–256, 1996.
Szczuciński, W., Zajączkowski, M. and Scholten, J.: Sediment accumulation rates in subpolar fjords – impact of post-Little Ice Age glaciers retreat, Billefjorden, Svalbard, Estuarine Coast. Shelf Sci., 85, 345–356, 2009.
Thorarinsdóttir, G. and Gunnarson, K.: Reproductive cycles of *Mytilus edulis* L. on the west and east coast of Iceland, Polar Res., 22, 217–223, 2003.
Walczowski, W. and Piechura, J.: New evidence of warming propagating toward the Arctic Ocean, Geophys. Res. Lett., 33, L12601, doi:10.1029/2006GL025872, 2006.
Walczowski, W. and Piechura, J.: Pathways of the Greenland Sea warming, Geophys. Res. Lett., 34, L10608, doi:10.1029/2007GL029974, 2007.
Walczowski, W., Piechura, J., Goszczko, I., and Wieczorek, P.: Changes in Atlantic water properties: an important factor in the European Arctic marine climate, ICES J. Mar. Sci., 69, 864–869, doi:10.1093/icesjms/fss068, 2012.
Wanner, H., Beer, J., Bütikofer, J., Crowley, T. J., Cubasch, U., Flückiger, J., Goosse, H., Grosjean, M., Joos, F., Kaplan, J. O., Küttel, M., Müller, S., Prentice, I. C., Solomina, O., Stocker, T. F., Tarasov, P., Wagner, M., and Widmann, M.: Mid- to late Holocene climate change: an overview, Quaternary Sci. Rev., 27, 1791–1828, 2008.
Weber, M. E., Niessen, F., Kuhn, G., and Wiedicke-Hombach, M.: Calibration and application of marine sedimentary physical properties using a multi-sensor core logger, Mar. Geol., 136, 151–172, doi:10.1016/S0025-3227(96)00071-0, 1997.
Werner, K., Spielhagen, R. F., Bauch, D., Hass, H. C., Kandiano, E. S., and Zamelczyk, K.: Atlantic Water advection to the eastern Fram Strait – multiproxy evidence for late Holocene variability, Palaeogeogr. Palaeocl., 308, 264–276, 2011.
Winkelmann, D. and Knies, J.: Recent distribution and accumulation of organic carbon on the continental margin west off Spitsbergen, Geochem. Geophy. Geosys., 6, Q09012, doi:10.1029/2005GC000916, 2005.

CPD
10, 3053–3095, 2014

Włodarska-Kowalczuk, M., Pawłowska, J., and Zajączkowski, M.: Do foraminifera mirror diversity and distribution patterns of macrobenthic fauna in an Arctic glacial fjord?, Mar. Micropaleontol., 103, 30–39, 2013.

Zajączkowski, M., Szczuciński, W., and Bojanowski, R.: Recent sediment accumulation rates in Adventfjorden, Svalbard, Oceanologia, 46, 217–231, 2004.

Zajączkowski, M., Nygård, H., Hegseth, E. N., and Berge, J.: Vertical flux of particulate matter in an Arctic fjord: the case of lack of the sea-ice cover in Adventfjorden 2006–2007, Polar Biol., 33, 223–239, 2010.

Zamelczyk, K., Rasmussen, T. L., Husum, K., Haflidason, H., de Vernal, A., Ravna, E. K., Hald, M., and Hillaire-Marcel, C.: Paleoceanographic changes and calcium carbonate dissolution in the central Fram Strait during the last 20 ka, Quaternary Res., 78, 405–416, 2012.

CPD
10, 3053–3095, 2014

Table 1. Water mass characteristics in Storfjorden and Storfjordrenna (Skogseth et al., 2005, modified). The two main water masses are in bold.

Watermass names	Watermass characteristics	
	Temperature (°C)	Salinity
Atlantic Water (AW)	**> 3.0**	**> 34.95**
Arctic Water (ArW)	**< 0.0**	**34.3–34.8**
Brine-enriched Shelf Water (BSW)	< −1.5	> 34.8
Surface Water (SW)	> 0.0	< 34.4
Transformed Atlantic Water (TAW)	> 0.0	> 34.8

CPD
10, 3053–3095, 2014

Table 2. AMS ^{14}C dates and calibrated ages.

Sample No	Depth (cm)	Lab No.	Raw AMS ^{14}C BP	Calibrated years BP $\pm 2\sigma$	Cal yr BP used in age model	Dated material
St 20A 5/6	5	Poz-46955	1835 ± 30 BP	1200–1365	1285	*Cilliatocardium cilliatum*
St 20A 39	38.5	Poz-46957	2755 ± 30 BP	2245–2470	Not used	*Astarte crenata*
St 20 78/79	78	Poz-46958	2735 ± 30 BP	2177–2429	2320	*Astarte crenata*
St 20 110	109.5	Poz-46959	3450 ± 30 BP	3079–3323	3220	*Astarte crenata*
St 20 142	141.5	Poz-46961	6580 ± 40 BP	6850–7133	6970	*Astarte crenata*
St 20A 152	151.5	Poz-46962	7790 ± 40 BP	8018–8277	8160	*Astarte crenata*
St 20 157	156.5	Poz-46963	8610 ± 50 BP	8989–9288	9120	*Bathyarca glacialis*
St 20 251/252/253	252	Poz-46964	10 200 ± 60 BP	10 886–11 223	11 140	*Thracia* sp.
St 20 396	395.5	Poz-46965	12 570 ± 60 BP	13 753–14 082	13 850	Bivalvia shell

CPD
10, 3053–3095, 2014

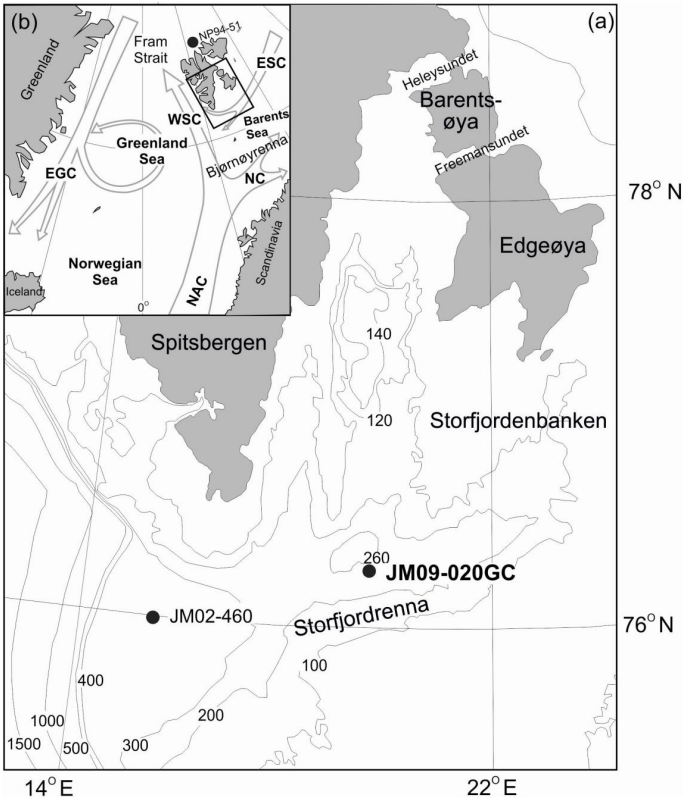

Figure 1. Location map **(a)** showing the core site from this study (JM09-020-GC) and core site of JM02-460 (Rasmussen et al., 2007). The inlet map **(b)** shows the modern surface oceanic circulation in Nordic Seas and location of a core NP94-51 (Ślubowska et al., 2005). Abbreviations: NAC – Norwegian-Atlantic Current; WSC – West Spitsbergen Current; ESC- East Spitsbergen Current; EGC – East Greenland Current; NC – Norwegian Current.

CPD
10, 3053–3095, 2014

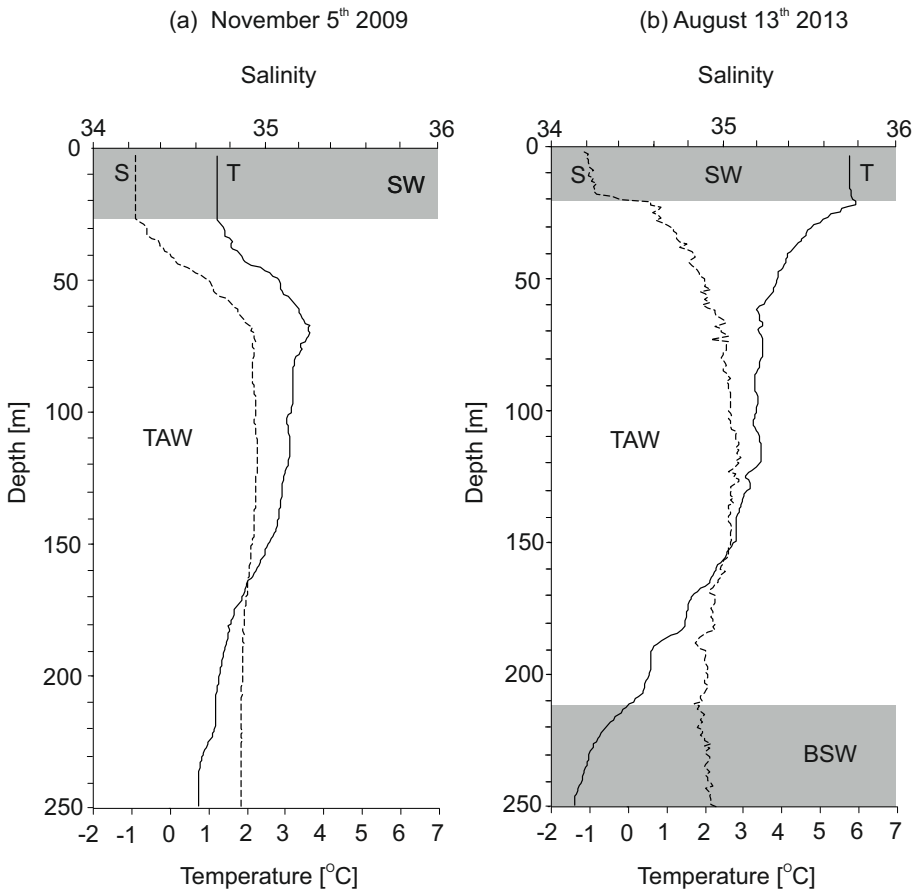

Figure 2. Temperature and salinity vs. depth, measured in 5 November 2009 **(a)** and in 13 August 2013 **(b)** at the site of core JM09-020GC. SW – Surface Water, TAW – Transformed Atlantic Water, BSW – Brine-enriched Shelf Water.

CPD
10, 3053–3095, 2014

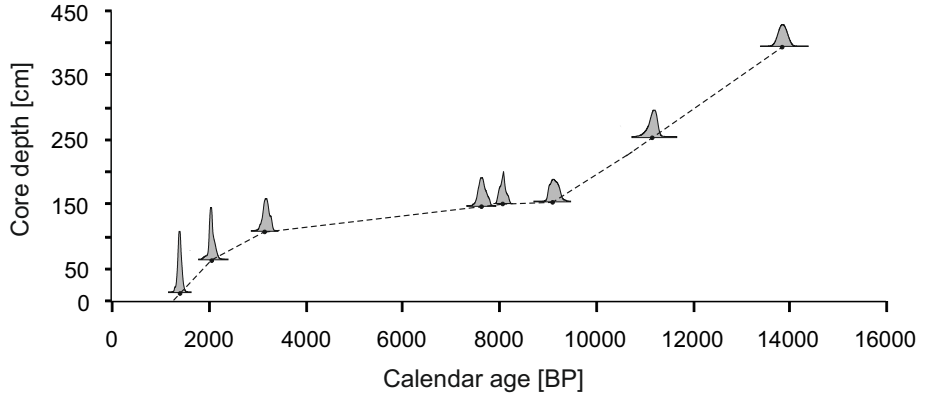

Figure 3. Age-depth relationship for JM09-020-GC based on 8 AMS ^{14}C calibrated ages with 2-sigma age probability distribution curves. The chronology is established by linear interpolation between the calibrated ages.

CPD
10, 3053–3095, 2014

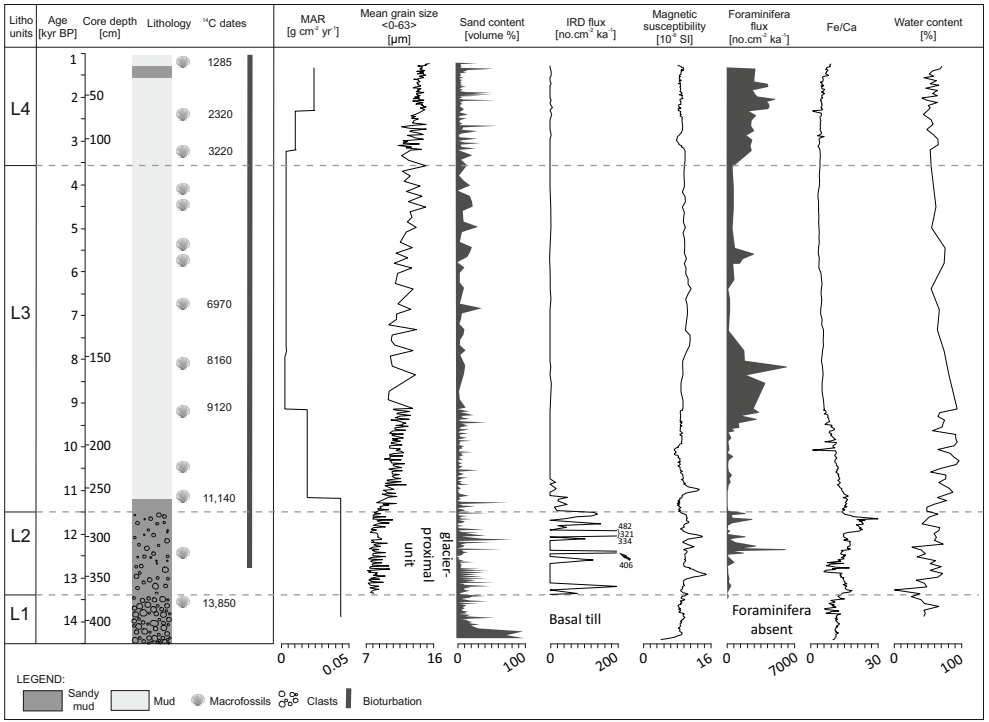

Figure 4. Lithological log of core JM09-020GC. Lithology, ^{14}C dates, occurrence of bioturbation, mass-accumulation rates, mean grain size in the range of 0–63 µm, sand content, ice-rafted debris flux, magnetic susceptibility, foraminifera flux as well as Fe/Ca ratio and water content. The results are presented with lithostratigraphic units (L1-L4), vs. calendar years (cal kyr BP) and core depth (cm).

CPD
10, 3053–3095, 2014

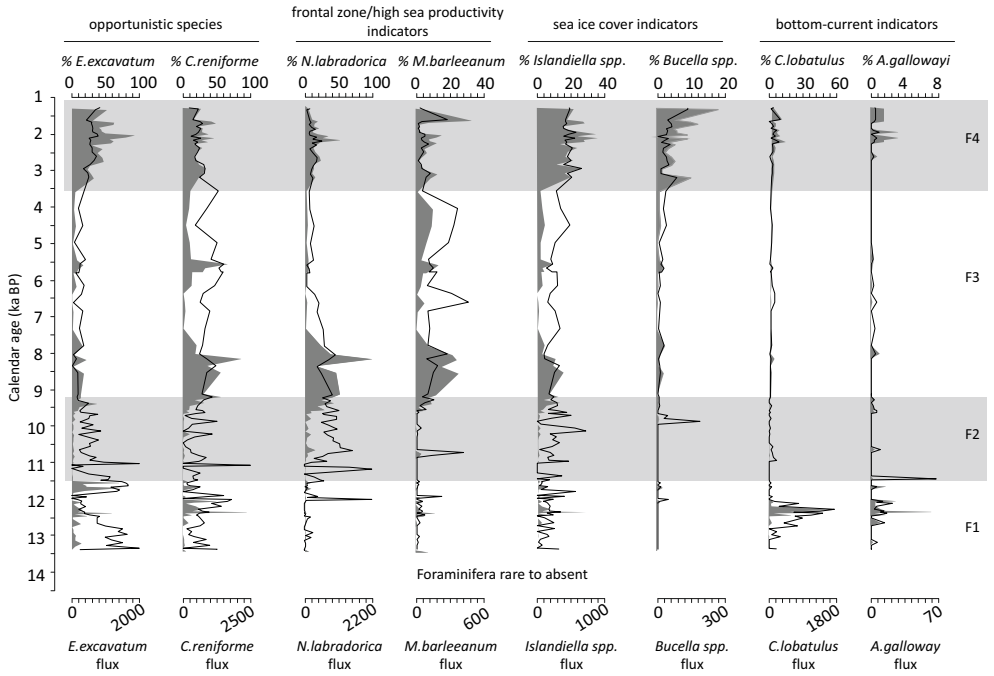

Figure 5. Percentage distributions (upper scale; black line) and fluxes (bottom scale; grey shading) of the most dominant benthic foraminiferal species plotted vs. thousands of calendar years with indicated foraminiferal zonation (zones F1–F4). Foraminiferal taxa are grouped based on their ecological tolerances described in the text.

CPD
10, 3053–3095, 2014

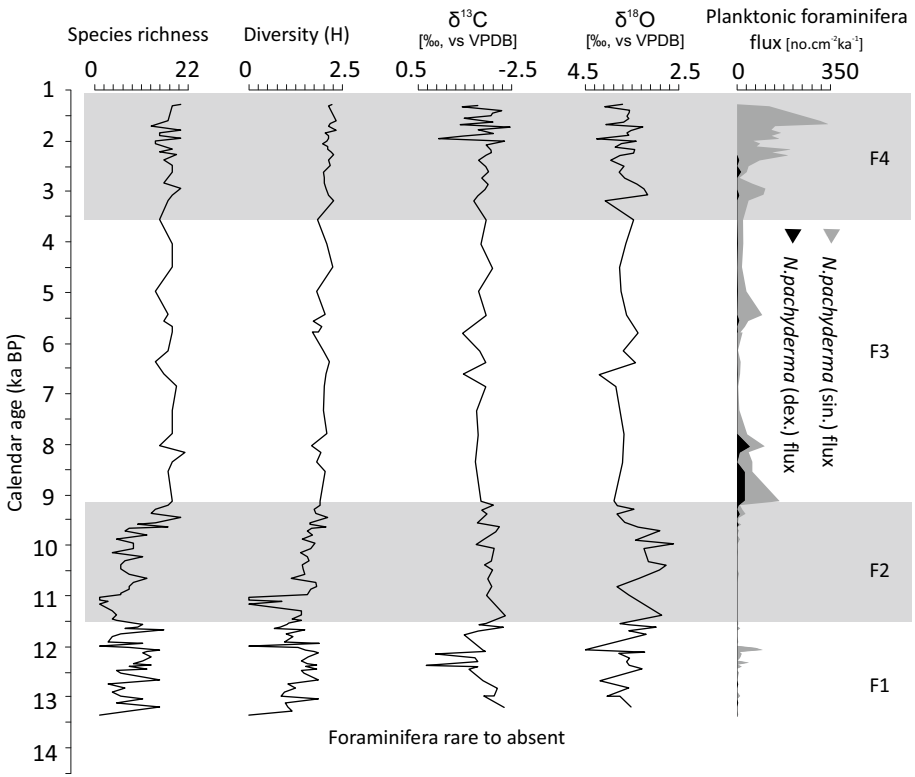

Figure 6. Diversity parameters (species richness and Shannon – Wiener index), stable oxygen and carbon isotope data (δ^{18}O and δ^{13}C), and flux of planktonic foraminifera (*Neogloboquadrina* spp.; over 90 % of the planktonic foraminifera assemblage) plotted vs. thousands of calendar years. The foraminiferal zonation (zones F1–F4) is indicated.

CPD
10, 3053–3095, 2014

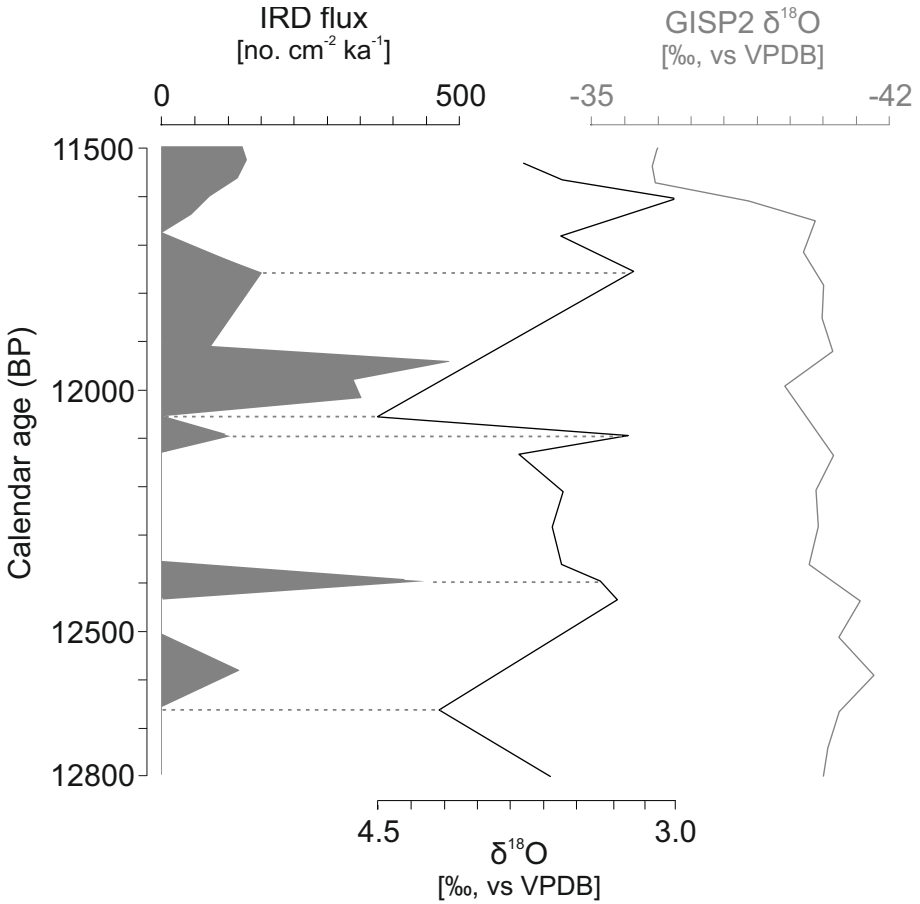

Figure 7. IRD flux (upper scale, grey shading) and oxygen stable isotopes records (bottom scale, black line) compared with oxygen stable isotopes records from ice core GISP2 from Greenland during the Younger Dryas period (12 800 cal yr BP to 11 500 cal yr BP).

CPD
10, 3053–3095, 2014

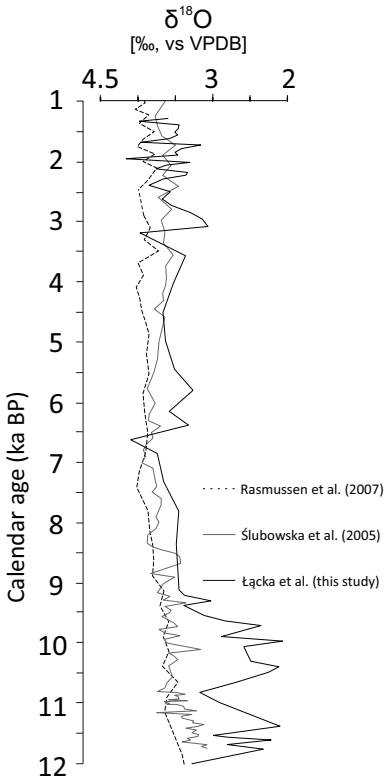

Figure 8. The comparison of δ^{18}O records (corrected for ice volume changes) between Łącka et al. (this study; black solid line) and Ślubowska et al. (2005; grey solid line) and Rasmussen et al. (2007; black dashed line) plotted vs. thousands of calendar years. The δ^{18}O records after Łącka et al. (this study) were measured on *E. excavatum* f. *clavata* and the two latter ones (Ślubowska et al., 2005 and Rasmussen et al., 2007) were measured on *M. barleeanum*.

CPD
10, 3053–3095, 2014

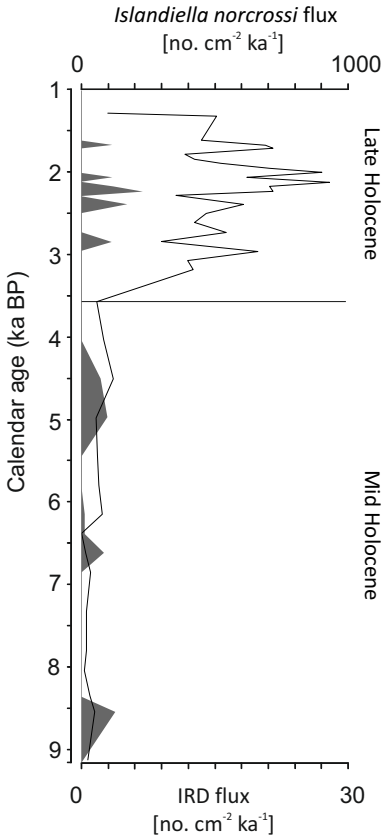

Figure 9. Fluxes of IRD (bottom scale; grey shading) and *Islandiella norcrossi* (upper scale; black line) plotted vs. thousands of calendar years. Both parameters may indicate the seasonal sea-ice cover (Polyak and Solheim, 1994; Hald and Steinsund, 1996) and that this has been particularly high during the past ca. 3600 years.

CPD
10, 3053–3095, 2014